Available online at www.sciencedirect.com
SCIENCE DIRECT®
Biochemical and Biophysical Research Communications 307 (2003) 355–361
BBRC
www.elsevier.com/locate/ybbrc

Cell shape provides global control of focal adhesion assembly

Christopher S. Chen,[a] Jose L. Alonso,[b,1] Emanuele Ostuni,[c,2] George M. Whitesides,[c] and Donald E. Ingber[b,*]

[a] *Departments of Biomedical Engineering and Oncology, Johns Hopkins University, Baltimore, MD 21205, USA*
[b] *Departments of Surgery and Pathology (Ingber Laboratory), Vascular Biology Program, Children's Hospital, Harvard Medical School, Enders 1007, 300 Longwood Avenue, Boston, MA 02115-5737, USA*
[c] *Department of Chemistry and Chemical Biology, Harvard University, Cambridge, MA 02138, USA*

Received 9 June 2003

Abstract

Cell spreading was controlled independently of the amount and density of immobilized integrin ligand by culturing cells on single adhesive islands of different sizes (100–2500 μm^2) and shapes (squares, circles, and lines) or on many smaller (3–5 μm diameter) circular islands that were coated with a saturating density of fibronectin and separated by non-adhesive regions. The amount of focal adhesions (FAs) containing vinculin and phosphotyrosine increased in direct proportion to cell spreading under all conditions. FAs localized asymmetrically along the periphery of the small islands that experienced highest tensional stress, and FA staining increased when cytoskeletal tension was stimulated with thrombin, whereas inhibitors of contractility promoted FA disassembly. Thus, these findings demonstrate the existence of an "inside-out" mechanism whereby global cell distortion produces increases in cytoskeletal tension that feed back to drive local changes in FA assembly. This complex interplay between cell morphology, mechanics, and adhesion may be critical to how cells integrate from and function in living tissues.

Cell adhesion to extracellular matrix (ECM) plays a critical role in many cellular functions, ranging from migration and proliferation to apoptosis [1,2]. The primary subcellular structures that mediate the regulatory effects of ECM adhesion on cell behavior are the focal adhesions (FAs). These macromolecular complexes mediate cell anchorage to ECM by physically coupling integrins to the contractile actin cytoskeleton [3,4]; they also orient and concentrate numerous signaling proteins at sites of integrin binding and clustering [3,5]. Because FAs function not only as the mechanical linkages that anchor the intracellular cytoskeleton to bound integrins and the ECM, but also as biochemical signaling hubs for many regulatory pathways, regulation of their assembly and disassembly is a critical mechanism for controlling cell function [1,4,6].

Early studies of cell adhesion on flat substrates described several distinct processes, including the initial clustering of integrins when they bind to ECM ligands, associated formation of FAs, and progressive maturation of these adhesion complexes as cells undergo active spreading and flattening. Because these processes proceed in parallel during initial attachment, it has been difficult to determine how each depends on the other. By varying the density of ECM ligand coated onto substrates, it was shown that FA formation and cell spreading both increase with increased integrin binding and clustering [7]. Studies have also suggested that cell shape depends on FA assembly, as knocking out FA proteins such as vinculin or focal adhesion kinase (FAK) results in cells that fail to spread normally [8,9]. Exposing suspended (round) cells to ECM-coated microbeads also induces FA formation within minutes [10,11], however, these structures appear to be more transient than the FAs formed on substrates. For example, ECM-coated beads only form mature, stable FAs if mechanical forces are applied to integrin-bound beads [12,13], and cells can generate such stabilizing forces at adhesions on planar

* Corresponding author. Fax: 1-617-232-7914.
E-mail address: donald.ingber@tch.harvard.edu (D.E. Ingber).
[1] Current address: Drug Discovery Department, PharmaMar S. A., Avda. de los Reyes, 1, 28770-Colmenar Viejo (Madrid), Spain.
[2] Current address: Surface Logix, Inc., 50 Soldiers Field Place, Brighton, MA 02135, USA.

0006-291X/03/$ - see front matter © 2003 Elsevier Inc. All rights reserved.
doi:10.1016/S0006-291X(03)01165-3

substrates through the action of their own contractile cytoskeleton [14,15]. Interestingly, we recently found that changes in cell shape may directly alter the magnitude of contractile forces that cells can exert on their adhesions [16,17], suggesting the possibility that the global shape of the cell (i.e., the degree to which it distorts) may feed back to regulate local FA formation at the cell base through this mechanoregulatory pathway.

We have previously developed a method to pattern ECM on surfaces to control cell shape while holding the ECM-coating density constant, as well as another strategy to control cell spreading independently of the total amount of ECM ligand that comes in contact with the cell [18,19]. In the present study, we use these approaches to vary endothelial cell shape and examine its effects on FA assembly. Our results show that the formation of stable FAs requires cell spreading and that this inside-out signaling is mediated by changes in mechanical forces exerted on integrin adhesion sites at the cell base.

Materials and methods

Cell culture. Bovine capillary endothelial (BCE) cells were cultured in standard growth media under 10% CO_2 on gelatin-coated tissue culture dishes in Dulbecco's modified Eagle's medium (DMEM) containing 10% calf serum, 2 mM glutamine, 100 μg/ml streptomycin, 100 μg/ml penicillin, and 1 ng/ml basic fibroblast growth factor (bFGF). Human endothelial cells (HMVEC) were cultured in endothelial basal medium (EBM; Clonetics) containing 10% fetal calf serum, 1 μg/ml hydrocortisone, 10 ng/ml epidermal growth factor (EGF), 10 μg/ml bovine brain extract, 50 μg/ml gentamycin, and 50 μg/ml amphotericin-B. Experiments with HMVECs were carried out in medium containing 2% serum; BCE cells were studied in defined medium containing DMEM supplemented with basic fibroblast growth factor (5 ng/ml), human high density lipoprotein (10 μg/ml), and transferrin (10 μg/ml).

Microfabrication of patterned substrates. Culture substrates were patterned with FN in islands such that the regions between the islands were not adhesive to cells, as previously described [18,20,21]. Briefly, microfabricated elastomeric stamps were used to print hexadecanethiol onto gold-coated cover glass and remaining spaces were coated with tri(ethylene glycol)-terminated alkanethiol. Substrates were immersed in 50 μg/ml of FN in PBS, rinsed with PBS, and handled using standard cell culture techniques. Hexadecanethiol was purchased from Aldrich and purified by silica gel column chromatography; the tri(ethylene glycol)-terminated alkanethiol was synthesized as described previously.

Immunofluorescence staining. Cultured cells were first permeabilized in a cytoskeletal stabilizing buffer (300 mM sucrose, 100 mM NaCl, 3 mM $MgCl_2$, 0.5% Triton X-100, and 10 mM Pipes, pH 6.8) [10], then fixed in 4% formaldehyde for 30 min, and washed in immunofluorescence buffer (IFB), containing 0.1% Triton X-100 and 0.1% BSA in PBS. The sample was incubated with primary antibody at 1 μg/ml in IFB for 1 h, washed, and incubated in fluorescent secondary antibody in IFB for 1 h and washed. Actin was stained with TRITC conjugated phalloidin (Sigma) in IFB for 1 h, and washed. Antibodies were obtained from commercial sources to recognize vinculin (Sigma), phosphotyrosine (UBI), talin (Sigma), paxillin (Sigma), FAK (Transduction Laboratories), αVβ3 integrin (Chemicon), and β1 integrin (Biosource). Secondary antibodies conjugated to Texas Red or FITC were obtained from Amersham and used at 1:40 dilution from stock.

Quantitation of cell shape and cell-ECM contact areas. Image processing software (BDS Image, Oncor) was used to calculate projected cell areas from images grabbed from the microscope through a CCD camera. Projected cell areas were determined from interactive tracing of cell edges of phase images. ECM contact areas were calculated in square micrometers based on intersection of images of direct fluorescence staining of ECM islands with projected cell areas.

Fluorescence quantitation of FA formation. The total amount of FAs formed per cell was measured using confocal microscopy to image cells stained by immunofluorescence for vinculin and phosphotyrosine. Images were taken at the plane of the cell–substrate interface, and quantified by integrating the pixel intensities across the area of a cell, defined by manually tracing the cell boundary. The signals were normalized to a standard sample that was used to calibrate the laser between each sample.

Results

To first examine whether cell shape might affect the extent of FA formation, square islands of different sizes were created on planar glass substrates (Fig. 1A) by microcontact printing self-assembled monolayers of the protein-adhesive alkanethiol, $HS(CH_2)_{15}CH_3$ in square forms; the areas between the islands were then filled in with a self-assembling, non-adhesive, and ethylene glycol-terminated alkanethiol. When the engineered substrates were incubated in a solution of FN, this ECM protein rapidly adsorbed only to the surface of the square islands and not to the surrounding regions (Fig. 1B). BCE cells plated on these substrates in defined medium containing saturating concentrations of growth factor selectively attached to the islands, and spread to take on the size and shape of the squares, ranging from 10 to 50 μm in side length (Fig. 1C). Thus, the degree of cell spreading and flattening was directly controlled by the size of the island, without varying the local density of FN in contact with cells.

To examine FA formation in cells spread to different degrees, samples were fixed, immunofluorescently probed for vinculin and phosphorylated tyrosine [10], and imaged using confocal microscopy. Qualitatively, vinculin staining appeared to be most prominent along cell borders regardless of island size (Fig. 1D). However, the punctate focal adhesions typically found underneath the central region of adherent cells only became prominent in cells that were spread on squares with sides of 40 μm or larger. When the amount of vinculin staining was quantified, we found that the amount of FA formation in cells correlated with the degree of cell spreading regardless of island size (Fig. 1E). Quantitation of phosphotyrosine within FAs indicated the existence of a similar correlation between the level of tyrosine kinase signaling within FAs and the extent of cell spreading (Fig. 1E).

Cells plated on larger islands were not only more spread, but they also came in direct contact with more immobilized FN due to the increased surface area covered. Thus, it remained unclear whether the increase in the total amount of FA per cell was a result of contact with more FN causing increased binding of integrins, or

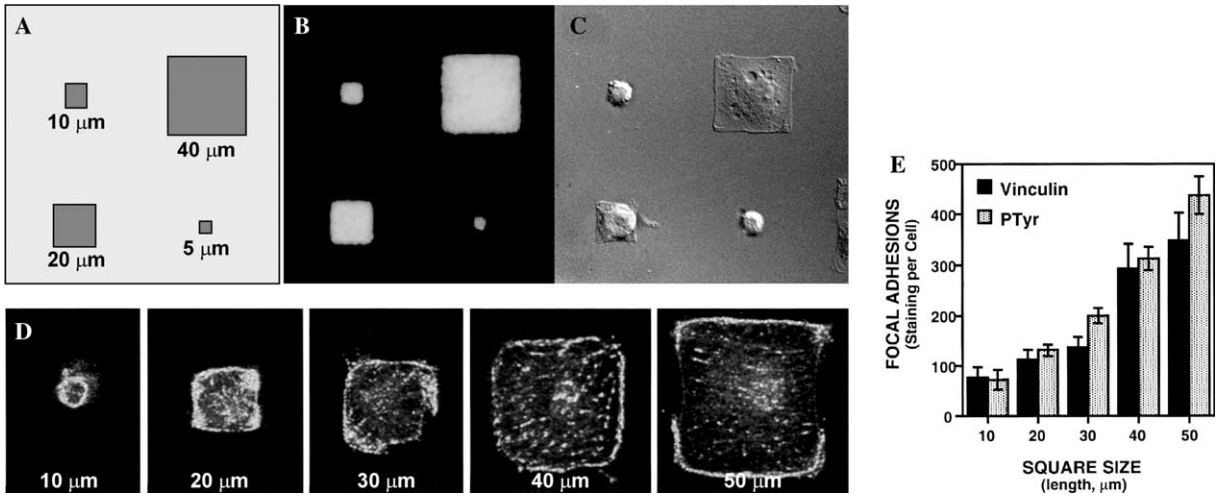

Fig. 1. Cell shape-dependent control of FA formation on micropatterned adhesive islands of different size coated with FN. (A) Diagram of an assortment of square adhesive islands with sides ranging from 10 to 50 μm in length that were micropatterned onto substrates using microcontact printing. (B) An immunofluorescence micrograph showing staining for adsorbed FN selectively limited to the square islands. (C) A differential interference contrast micrograph of BCE cells cultured on different sized, square FN islands. (D) Fluorescent confocal micrographs of individual, vinculin-labeled cells cultured on square islands of different sizes (lengths of sides are indicated). (E) Quantitation of total vinculin and total phosphotyrosine labeling per cell, for cells cultured on different sized squares. Over 30 cells per condition were averaged; error bars indicate standard error of the mean.

a result of changes in cell shape and intracellular structure. To distinguish these two possibilities, cells were seeded onto closely spaced subcellular-scale islands (again separated by non-adhesive regions) such that single cells could spread across multiple islands. Using this approach to change the size and spacing of the islands, we could vary cell spreading while maintaining the total area of cell-FN contact constant (Fig. 2A). In all experiments, the local molecular ECM coating density also remained constant, and at a level that would optimally promote cell spreading on unpatterned substrates (Fig. 2A, bottom). When BCE cells were plated on substrates containing 20 μm or larger spaces between islands, they remained on single islands, whereas cells on islands spaced 10 μm or less consistently spread across multiple islands. When the island spacing was decreased further, cell spreading continued to increase. Immunofluorescence studies revealed that vinculin-containing FAs preferentially localized along the circumference of the subcellular-sized islands and coalesced to form larger, more intensely fluorescent FAs as compared to those observed within control cells cultured on unpatterned substrates (Fig. 2A, right). Furthermore, the circumferential localization of vinculin around these islands was not symmetric. Most notably, the FAs that formed on 3 μm diameter islands formed horseshoe-like structures where the brightest staining faced away from the centroid of the cell.

Using this method, three island coating patterns (3, 5, and 10 μm circular islands) were chosen such that cell spreading could be varied more than ten fold, even though the cells came in contact with the same total amount of FN per cell (Fig. 2B). The amount of FAs formed in each cell under different spreading conditions was quantified using confocal microscopy to measure the total area of vinculin and phosphotyrosine staining per cell. The total FA area formed per cell increased directly as cell spreading was promoted, though the amount of ECM per cell was held constant (Fig. 2B). To confirm this finding, a second series of patterns containing parallel lines of similar widths and spacings (3–10 μm line widths and 5–20 μm spacings) was used to promote cell spreading without varying cell-ECM contact area. Again, FAs formed in proportion to the degree at which cells spread across the substrate. When all of the data for vinculin and phosphotyrosine per cell obtained from cells cultured on the different shaped islands used in this study (squares, circles, and lines) were pooled and plotted as a function of ECM-cell contact area or cell spreading area, no correlation between total ECM amount and FA area could be demonstrated (not shown). In contrast, the projected cell area correlated directly with the total area of FA formed per cell as well as the total amount of phosphotyrosine staining (Fig. 2C).

The FAs that formed when cells were plated on 3 and 5 μm circles, and contained both vinculin and phosphotyrosine, appeared significantly brighter and larger than FAs formed in cells cultured on control, unpatterned substrates. To confirm that these structures were FAs, cells were stained for many other proteins found within FAs, including paxillin, talin, FAK, and integrins $\alpha5\beta1$ and $\alpha V\beta3$. In all cases, like vinculin, these FA proteins were found in the ring-like structures oriented

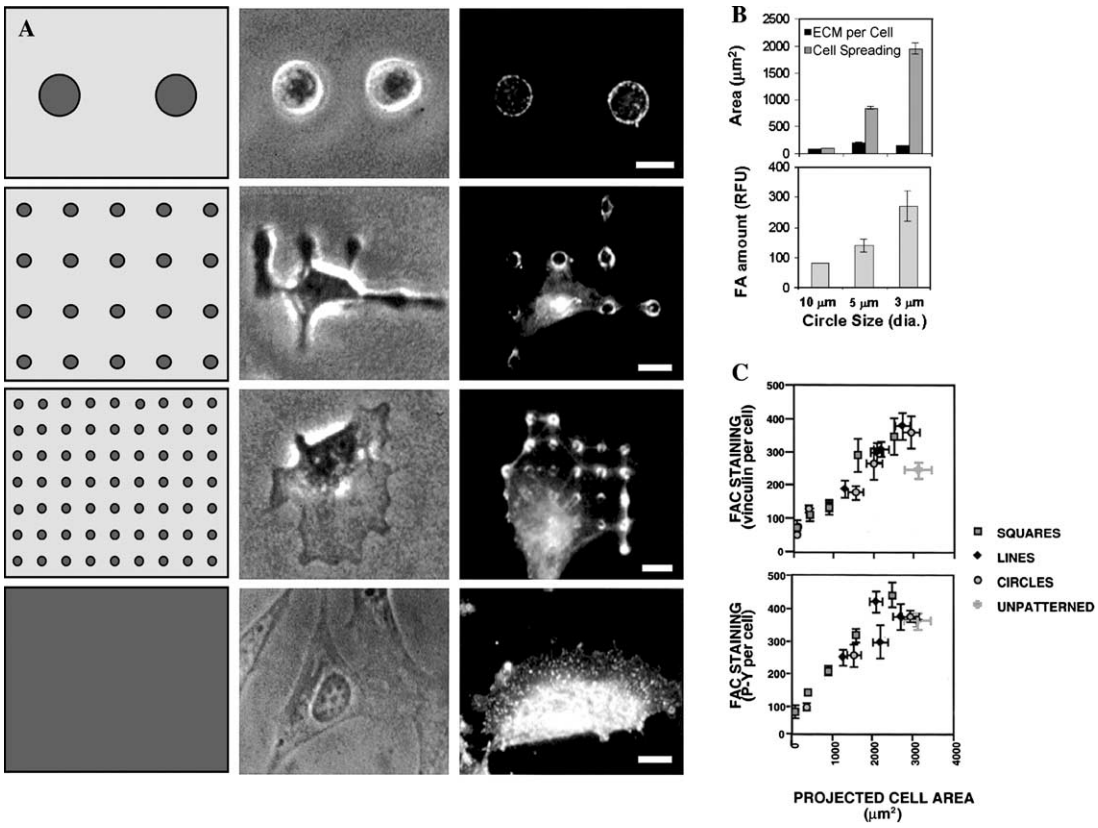

Fig. 2. FA formation increases as cell spreading is promoted. (A) Diagrams of adhesive patterns (left), phase contrast images of cells (middle), and immunofluorescence images of vinculin in a series of micropatterned substrates where single cells can spread across multiple, small adhesive islands. The bottom row shows a cell on an unpatterned FN substrate. Scale bars indicate 10 μm in length. (B) Quantitation of total contact area of FN per cell (ECM per cell), projected cell area (cell spreading), and amount of vinculin per cell on three different micropatterned substrates containing 3, 5, or 10 μm circular islands. (C) Quantitation of total vinculin and phosphotyrosine per cell plotted against projected area of cells for cells cultured on many different micropatterned geometries, including squares, circles, lines, and unpatterned substrates.

along the periphery of the FN islands (Fig. 3). Double-labeling experiments also confirmed that the different FA proteins co-localized in similar locations (Fig. 3). Again, these ring-like structures were asymmetric and appeared to stain most intensely on the distal side of the islands (i.e., relative to the cell center).

FA assembly can be modulated by the level of tensional forces that are transmitted across integrin recep-

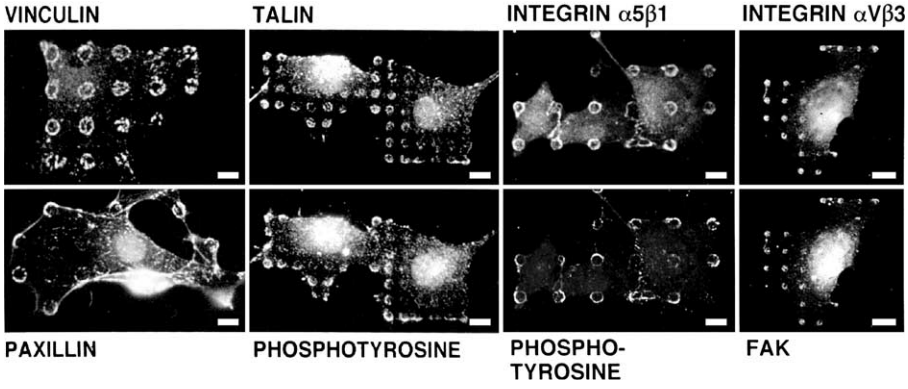

Fig. 3. Distribution of focal adhesion components in cells cultured on substrates micropatterned with small (3 and 5 μm) FN islands. Cells were immunostained for vinculin, paxillin, talin, phosphotyrosine, FAK, and integrins α5β1 and αVβ3. Both single (vinculin and paxillin) and double (talin vs. phosphotyrosine, integrin α5β1 vs. phosphotyrosine, and integrin αVβ3 vs. FAK) immunofluorescence images demonstrated localization of FA components to the periphery of these FN islands. Scale bars indicate 10 μm in length.

tors [15,22] and tractional forces exerted by the cytoskeleton are directed from the periphery towards the cell center [12,14]. Thus, one possibility for this asymmetric localization of FAs in the present study is that intracellular mechanics may alter the architecture of the adhesions: tension may be greater at the distal side of the FAs compared to its proximal side. While immunofluorescence studies revealed that neither microtubules nor intermediate filaments localized to these FAs, the distribution of actin stress fibers (as visualized by rhodaminated-phalloidin labeling) was dramatically altered by the artificial geometry of the surface (Fig. 4). Stress fibers were anchored at the periphery of islands where FAs formed and stretched from island to island across non-adhesive regions as if they mapped out tension field lines within the cytoskeleton. Confocal microscopy of FAs double stained for vinculin and F-actin confirmed that these cytoskeletal filaments inserted in a crescent only on the distal side of the 3 μm circles (Fig. 4). Thus, the site of greatest tensional stress application, as implied by the position of the actin stress fibers, correlated closely with the asymmetric distribution of FAs around these islands (Fig. 3). These results suggested that cell shape may modulate FA formation by controlling the amount of cytoskeletal tension that is exerted on integrin receptors bound to immobilized FN at the cell base.

To test directly whether the assembly and asymmetric shape of these FAs were sensitive to changes in cytoskeletal tension, BCE cells spread across 5 μm diameter islands were exposed to inducers and inhibitors of actomyosin-based tension generation. Control (untreated) cells again formed FAs that were more intensely stained distally on the islands (Fig. 5A). The addition of thrombin, a potent vasoconstrictor, caused a dramatic increase in total FA staining on the islands (Fig. 5B) as more of the island became mechanically engaged, and the asymmetry of the staining pattern intensified. To examine this effect more closely, we examined this effect of cytoskeletal tension on FAs using the much larger HMVECs. Again, FA staining was restricted to the circumference in control cells (Fig. 5E) and intensified with the addition of thrombin (Fig. 5F). In these cells, the tension-dependent intensification clearly illustrates that the degree of asymmetry and circumferential localization of the FAs is driven by cytoskeletal tension. In contrast, 2,3-butanedione monoxime (BDM) and KT5926, inhibitors of myosin-activated contractility that act via distinct mechanisms, induced almost

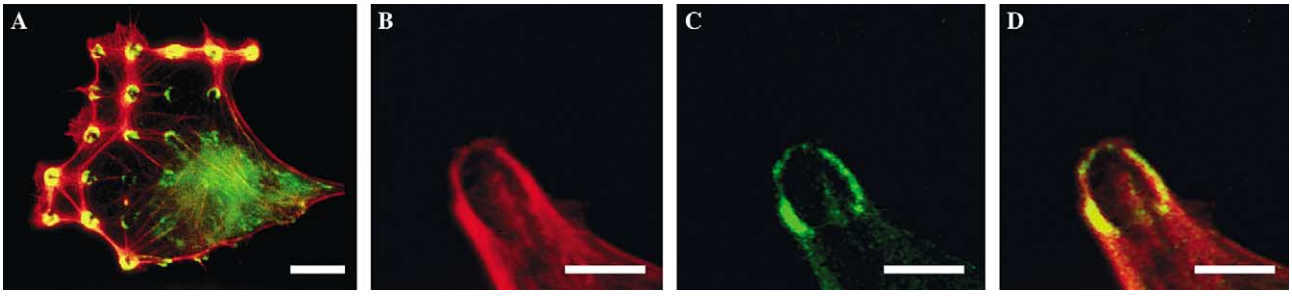

Fig. 4. Structural asymmetry within FAs on micropatterned substrates. (A) Immunofluorescence image of F-actin (red) and vinculin (green) in a BCE cell cultured on 3 μm diameter FN islands. Scale bar indicates 10 μm in length. (B–D) High magnification confocal images of a single FA formed on one FN island, showing F-actin (B), vinculin (C), and combined staining (D). Scale bars indicate 3 μm in length.

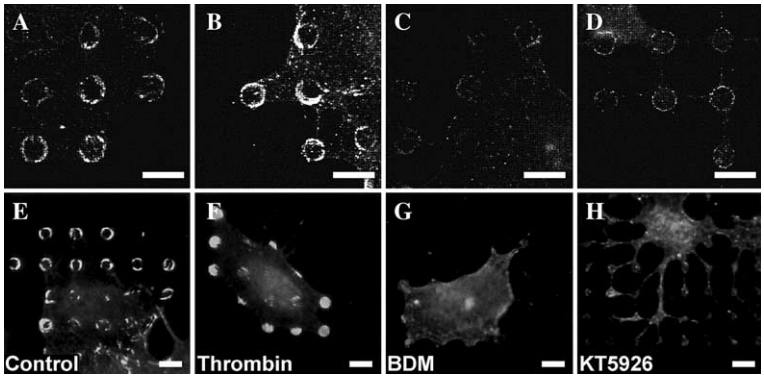

Fig. 5. Mechanical tension in the cytoskeleton modulates FA amount and structure. Immunofluorescence images of vinculin in BCE (A–D) and HMVEC (E–H) cells on 5 μm islands that were untreated (A,E) or exposed to thrombin (B,F), BDM (C,G), or KT5926 (D,H). Scale bars indicate 10 μm in length.

complete FA disassembly in both BCEs (Figs. 5C and D) and HMVECs (Figs. 5G and H). Interestingly, these inhibitors also reduced the asymmetry previously observed in untreated cells, although the FA staining still remained limited to the periphery of the islands. These results show that the size and position of FAs are modulated by both the level and direction of intracellular forces.

Discussion

By using a microprinting approach to vary the geometry of cell–substrate interactions and thereby control cell shape, we have identified a previously unrecognized causal relationship between ECM, cell shape, and FA regulation. In general, it is assumed that FA assembly is controlled by clustering of integrin receptors induced by binding to immobilized ECM ligands, and that FA formation is then necessary for cell spreading. In contrast, in the present study we show that FA assembly can be varied independently of the total amounts of ECM binding, and instead, that it scales directly with cell spreading. Importantly, when cells spread to the same degree had different amount of ECM beneath them (e.g., cells on single islands vs. on multiple dots), the FA quantity per cell was not significantly different. Thus, although ECM binding is required for FA formation, neither binding to a high density of immobilized ECM ligand nor to a large amount of ECM is sufficient to promote FA assembly. Taken together, these results demonstrate that FA formation is also governed by changes in internal cytoskeletal structure and mechanics that result from large-scale changes in cell shape (i.e., cell distortion).

The mechanism by which cell shape regulates FA formation was suggested by previous studies which showed that cytoskeletal tension and mechanical stress directly affect FA assembly [12,14,15,23]. However, while past studies implied that mechanical stresses applied directly to integrins modulate associated FA assembly, our results demonstrate that the global shape of cells and their internal cytoskeletal structure play an important role in constraining the magnitude, distribution, and direction of such stresses across the cell surface, and thereby control local FA assembly and organization. In fact, the asymmetric structure of the FAs on small islands correlated directly with the tension field patterns and distribution of actin filament staining. FA formation also could be increased or decreased by raising or lowering cytoskeletal tension, respectively, using pharmacological agents. Moreover, the horseshoe-like distribution of FAs on the subcellular-sized, circular islands appeared to be polarized in the axis of the overlying stress fibers, and exaggerated when tension was increased. Conversely, inhibiting actomyosin tension decreased FAs significantly, and abolished the horseshoe polarity. But even in these non-contractile cells, FAs appeared as faint symmetric hollow rings, rather than be evenly distributed across the entire island, again confirming that integrin contact with ECM alone is not sufficient to explain FA formation. Taken together with recent work demonstrating that cell shape can regulate the magnitude of contractile force generated in cells [16,17], these findings suggest that mechanical tension in the cytoskeleton, rather than ECM presentation, molds the shape and distribution of FAs.

Past studies have demonstrated that many fundamental biological processes, such as growth, differentiation, migration, and apoptosis, are mediated by changes in cell shape and cytoskeletal integrity [1,2]. Here, we identify the existence of a control mechanism whereby cell shape also regulates the quantity, size, and organization of FAs, and we show that this is mediated through changes in cell contractility. Because FAs contain signaling components from a large number of signaling cascades [1,24], shape-regulated FA formation could provide a molecular mechanism for how cell structure and physical distortion of cell shape can be transduced into biochemical signals inside the cell. Thus, this inside-out regulation of FA assembly may be critical in integrating many physical cues—cell shape, ECM compliance, intracellular tension, and cytoskeletal architecture—into the signals that drive cell function.

Acknowledgments

This work was made possible by funding from NIH grants CA45548 (D.E.I.) and GM30367 (G.M.W.). Microfabrication was carried out with the assistance of the Material Research Science and Engineering Center of Harvard University. We also would like to thank Bob Ezzell for his assistance with confocal microscopy.

References

[1] M.A. Schwartz, M.H. Ginsberg, Nat. Cell Biol. 4 (2002) E65–68.
[2] N. Boudreau, M.J. Bissell, Curr. Opin. Cell Biol. 10 (1998) 640–646.
[3] S.K. Sastry, K. Burridge, Exp. Cell Res. 261 (2000) 25–36.
[4] N. Wang, J.P. Butler, D.E. Ingber, Science 260 (1993) 1124–1127.
[5] F.J. Alenghat, D.E. Ingber, Sci. STKE 2002 (2002) PE6.
[6] B. Geiger, A. Bershadsky, Cell 110 (2002) 139–142.
[7] S.P. Massia, J.A. Hubbell, J. Cell Biol. 114 (1991) 1089–1100.
[8] R.M. Ezzell, W.H. Goldmann, N. Wang, N. Parasharama, D.E. Ingber, Exp. Cell Res. 231 (1997) 14–26.
[9] J.D. Owen, P.J. Ruest, D.W. Fry, S.K. Hanks, Mol. Cell. Biol. 19 (1999) 4806–4818.
[10] G. Plopper, D.E. Ingber, Biochem. Biophys. Res. Commun. 193 (1993) 571–578.
[11] S. Miyamoto, H. Teramoto, O.A. Coso, J.S. Gutkind, P.D. Burbelo, S.K. Akiyama, K.M. Yamada, J. Cell Biol. 131 (1995) 791–805.
[12] C.G. Galbraith, K.M. Yamada, M.P. Sheetz, J. Cell Biol. 159 (2002) 695–705.

[13] C.J. Meyer, F.J. Alenghat, P. Rim, J.H. Fong, B. Fabry, D.E. Ingber, Nat. Cell Biol. 2 (2000) 666–668.
[14] N.Q. Balaban, U.S. Schwarz, D. Riveline, P. Goichberg, G. Tzur, I. Sabanay, D. Mahalu, S. Safran, A. Bershadsky, L. Addadi, B. Geiger, Nat. Cell Biol. 3 (2001) 466–472.
[15] D. Riveline, E. Zamir, N.Q. Balaban, U.S. Schwarz, T. Ishizaki, S. Narumiya, Z. Kam, B. Geiger, A.D. Bershadsky, J. Cell Biol. 153 (2001) 1175–1186.
[16] N. Wang, E. Ostuni, G.M. Whitesides, D.E. Ingber, Cell Motil. Cytoskel. 52 (2002) 97–106.
[17] J.L. Tan, J. Tien, D.M. Pirone, D.S. Gray, K. Bhadriraju, C.S. Chen, Proc. Natl. Acad. Sci. USA 100 (2003) 1484–1489.
[18] C.S. Chen, M. Mrksich, S. Huang, G.M. Whitesides, D.E. Ingber, Science 276 (1997) 1425–1428.
[19] K.K. Parker, A.L. Brock, C. Brangwynne, R.J. Mannix, N. Wang, E. Ostuni, N.A. Geisse, J.C. Adams, G.M. Whitesides, D.E. Ingber, FASEB J. 16 (2002) 1195–1204.
[20] R. Singhvi, A. Kumar, G.P. Lopez, G.N. Stephanopoulos, D.I. Wang, G.M. Whitesides, D.E. Ingber, Science 264 (1994) 696–698.
[21] C.S. Chen, E. Ostuni, G.M. Whitesides, D.E. Ingber, Methods Mol. Biol. 139 (2000) 209–219.
[22] D. Choquet, D.P. Felsenfeld, M.P. Sheetz, Cell 88 (1997) 39–48.
[23] M. Chrzanowska-Wodnicka, K. Burridge, J. Cell Biol. 133 (1996) 1403–1415.
[24] D.E. Ingber, J. Cell Sci. 116 (2003) 1397–1408.